



Forming characteristics of additive manufacturing process by twin electrode gas tungsten arc

QingLin Han¹ · Dayong Li² · Haojun Sun¹ · Guangjun Zhang¹

Received: 5 March 2019 / Accepted: 14 August 2019 / Published online: 26 August 2019
© Springer-Verlag London Ltd., part of Springer Nature 2019

Abstract

Traditional gas tungsten arc-based additive manufacturing (GTA-AM) system normally applies high-level deposition current to achieve a high deposition rate. Due to the induced high arc pressure, defects (e.g., humps) may always happen, which made the deposited beads unsuitable for additive manufacturing (AM) purposes. To solve this issue, a twin electrode approach has been applied in an implemented GTA-AM system, which achieved high deposition rate while kept the arc pressure with a relatively small value. The objective of this paper is to investigate the principles of using the twin electrode GTAW approach in an AM context. This paper first explored the maximum allowable wire feed speed (MAWFS) with regard to the deposition currents ranging from 200 to 450 A. A piecewise linear model was established to represent the relationship between the MAWFS and the current, which formed a basis for defining the feasible range of travel speed at a given deposition current. To validate the proposed principles, a case study was conducted, in which a set of deposition parameters were determined for fabricating a cube part. The deposition rate of twin electrodes GTA-AM is up to 2.7 kg/h, which is almost twice as much as that of traditional GTA-AM.

Keywords Additive manufacturing · Twin electrode gas tungsten arc · Forming characteristics · Deposition rate

1 Introduction

Additive manufacturing (AM) is a near-net shaping technology for fabricating parts directly from the CAD model. Compared with the traditional manufacturing technologies such as turning and milling, AM was considered as a promising approach with many advantages, such as less procedure, higher flexibility, and higher material utilizing rate. Wire and arc additive manufacturing (WAAM) employs the arc as the heat source to melt fed wire, which is proved to be an effective approach for depositing metal parts with a moderate complexity [1]. In the literature, many WAAM systems have been implemented in the recent decade. For instance, Ma et al. [2] developed a hybrid manufacturing system, which jointly applied subtractive manufacturing and additive manufacturing to fabricate

large thin-walled aluminum structures. Williams et al. [3] developed a WAAM system, which supports fabrication of aircraft parts with a large size, e.g., wing spar and external landing gear. In the work of Li et al. [4], inclined multilayer multibead steel parts were deposited by using a robotic WAAM system. Recently, the WAAM was applied as the main enabler for repairing surface defects of metal parts [5].

According to the power source and wire-feeding mode, WAAM can be classified as gas tungsten arc additive manufacturing (GTA-AM) and gas metal arc additive manufacturing (GMA-AM). In comparison with GMA-AM, the deposition process of GTA-AM is more stable since the wire-feeding process is independent of the arc length. Various metallic materials can be deposited by using GTA-AM, including steel, nickel alloy, aluminum alloy, and titanium alloy. [6]. Wang et al. [7] deposited a Ti-6Al-4 V thin-wall structure by GTA-AM and tested the microstructure and mechanical properties of the fabricated structure. Bai et al. [8] investigated the thermal cycles of the GTA-AM deposition process for 2219 aluminum alloy and reported the diversity of microstructure at different positions of the deposition structure. Geng et al. [9] analyzed the droplet transfer type of GTA-AM in order to optimize the wire feed angle and to prevent the formation of the gap defects between deposition beads.

✉ Guangjun Zhang
zhanggj@hit.edu.cn

¹ State Key Laboratory of Advanced Welding and Joining, Harbin Institute of Technology, West Straight street 92, Harbin 150001, People's Republic of China

² Bohai Shipyards Group Co., Ltd, Huludao 125000, People's Republic of China

Among the abovementioned research efforts with regard to the GTA-AM, the deposition rate of fed material was less than 1.5 kg/h [10], which confined its application in fabrication of large-scale parts. During the GTA-AM process, the molten pool is formed by the heating of the arc. The fed wire was melted into droplets by the arc and fed into the molten pool to form a deposited bead. The deposition rate is dependent on the melting speed of the fed wire [11]. Accordingly, to improve the deposition rate, it is necessary to increase the arc heat input and to feed more wire [12].

Increasing the deposition current is a common way to provide more heat input, as a result, a high deposition rate can be achieved. However, since traditional GTA-AM system employs a single tungsten electrode, the arc pressure will rise rapidly with the growth of deposition current [13]. The increased arc pressure has a great impact on the flowing state of the molten pool, which produces many types of forming defects, such as undercutting and humping. To avoid the formation of such defects, the deposition current of traditional GTA-AM was limited to a small value (usually less than 200A). Therefore, deposition of well-formed bead with a high deposition current by GTA-AM is one of the research hotspots.

In the welding field, Kobayashi et al. [14] proposed the twin electrode gas tungsten arc welding technology and applied it to construct large storage tanks. This approach employed two independent electrodes insulated from each other in one torch. Every electrode was connected to a GTAW power supply. The two sub-arcs generated by the two electrodes could attract each other by Lorentz force, forming a coupled arc [15]. Leng et al. [16] studied the physics characteristics of this coupled arc and reported that the arc pressure of the coupled arc was lower than that of the conventional gas tungsten arc with the same welding parameters. Wang et al. [17] investigated the behavior of the coupled arc plasma and molten pool by numerical simulation and analyzed the weld bead penetration. It can be concluded from the related work that the twin electrode GTA approach enables a high deposition rate of the fed material, which has many potentials for AM purposes.

In the context of AM, the forming appearance of the deposited beads is a crucial factor that influences the quality of the fabricated part. Accordingly, it is necessary to investigate the forming characteristics of beads under varied manufacturing parameters of twin electrode GTA-AM. This paper aims at improving the deposition rate of GTA-AM by employing the twin electrode gas tungsten arc as the heat source. To this end, the forming characteristics of beads deposited using high deposition currents (up to 450 A) were investigated, and the process window for producing well-formed beads was proposed. Section 2 introduces the implemented system and the applied methods. Section 3 presents the experimental results and findings.

Section 4 validates the feasibility of fabricating metal components with twin electrode GTA-AM. The main conclusions of this paper are given in Section 5.

2 Experimentation overview

2.1 Experimental system

An overview of the developed twin electrode GTA-AM system is shown in Fig. 1. It contains a motion platform, a twin electrode arc welding torch, and two Rilon WS-400 GTAW power machines, a BY1 wire feeder, a computer, and a signal transmission module. The motion platform has 4 degrees of freedom (DOF) including 3 translational DOF along *X*-axis, *Y*-axis, *Z*-axis, and 1 rotational DOF around *Z*-axis. The twin electrode arc welding torch was water-cooled and had two mutual insulated tungsten electrodes central symmetrically fixed in it. The distance between the tungsten electrode tips was 1.5 mm. The positive electrodes of the GTAW power machines were fixed to the substrate, while the negative electrodes of the GTAW power machines were connected to the corresponding tungsten electrodes. Two independent current circuits were formed.

The wire was always fed to the forward position of the molten pool through a nozzle fixed in front of the torch. The computer is the control center of the system for setting the velocity of the travel speed of welding torch, striking or extinguishing the arc, adjusting the deposition current and wire feed speed, and showing the status information of the deposition process through a human-machine interface. It also supports reading and running the deposition job programs written according to the time sequence of deposition parameters.

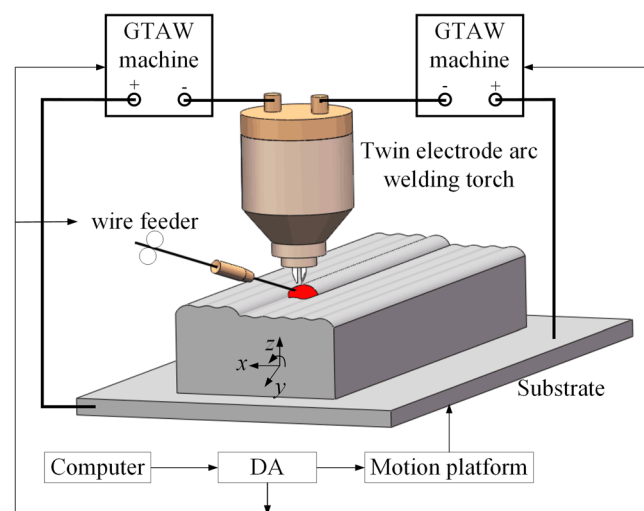


Fig. 1 Schematic diagram of twin electrode GTA-AM system

2.2 Materials

In this work, a 1.2-mm diameter H08Mn2Si steel wire was employed as filling material deposited on a 300*150*10-mm Q235 mild steel substrate. The chemical constituent of the wire and the substrate are shown in Table 1. The twin electrodes were 3.0-mm diameter cerium tungsten sticks. The electrodes were milled to the slanting shape with the tip angle of 30 deg. During the deposition process, the twin electrode distribution was always perpendicular to the deposition direction. The shielding gas was Ar.

2.3 Experimental procedure

The deposition parameters of twin electrode GTA-AM include deposition current, travel speed, wire feed speed, arc length, wire feed angle, and shielding gas flow. In the conducted experiments, the twin electrodes were loaded with the same current. It implies that the overall deposition current was as twice as the current flowing through every electrode. This paper mainly investigated the influence of the first three factors on the forming characteristics of deposition beads, because they are the main deposition parameters of GTA-AM. The other factors were fixed as constant. The considered values and ranges of the deposition parameters are listed in Table 2.

In order to get the process window of twin electrode GTA-AM, the single-bead deposition experiments were designed in two stages. The objective of the first stage was to establish the correlation between the deposition current and its maximum allowable wire feed speed. Since twin electrode GTA-AM striving after a high deposition rate, it is necessary to feed as much wire as possible in the premise of depositing the well-formed bead. Thus, the maximum allowable wire feed speed at each deposition current was explored.

The specific settings of the experiments are detailed as follows: the applied deposition current started from 200 A with an increment of 50 A until maximum allowable wire feed speed reached the upper limit of the wire-feeding machining (5 m/min). For each deposition current, the beads were deposited with different wire feed speeds and the same travel speed until serious forming defects appeared on the surface of the deposited beads.

The objective of the second stage was to explore the travel speed ranges that enable obtaining well-formed beads. According to the result of the first stage, the maximum

Table 1 Chemical constituent of the substrate and wire (wt. %)

Elements	C	Mn	Si	S	P
Q235	0.12~0.20	0.30~0.70	≤ 0.30	≤ 0.045	≤ 0.045
H08Mn2Si	0.06~0.15	1.40~1.85	0.80~1.15	≤ 0.025	≤ 0.025

Table 2 Experimental condition of twin electrode GTA-AM

Parameter	Value of ranges
deposition current (A)	200–450
Wire feed speed (m/min)	0–5
Travel speed (mm/s)	0–10
Ar gas flow (L/min)	11
Arc length (mm)	5
Wire feed angle (deg)	20
Initial temperature (°C)	< 50

allowable wire feed speed was set as the wire feed speed in the second stage. The forming characteristics of deposited beads were evaluated based on a consideration of their forming appearance and cross-sectional profiles. The data with regard to the cross-sectional profile of beads was aggregated by a META SLS-050 line-structured laser sensor with the measurement accuracy of 0.05 mm. The line-structured laser was vertically projected on the surface of the beads, as shown in Fig. 2a. The aggregated original image and the point cloud data after image processing were shown in Fig. 2b and c, respectively.

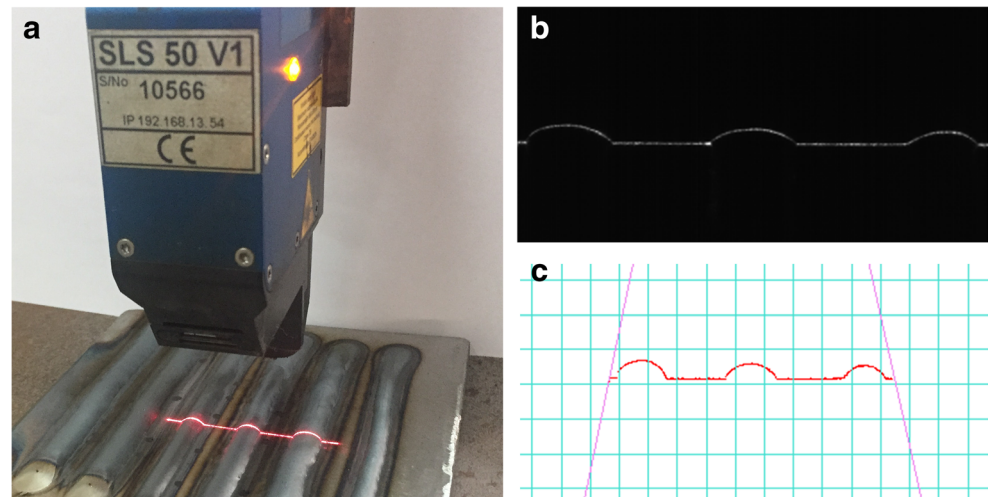
3 Results and discussion

3.1 The maximum allowable wire feed speed at each deposition current

The experiments were done as Table 3, and some typical deposition beads were shown as Fig. 3. The outlines of the beads deposited by the current of 250 A at different wire feed speeds were shown in Fig. 4. In general, the twin electrode GTA-AM technology has the ability to deposit the well-formed beads with the deposition current from 200 to 450 A while the traditional GTA-AM usually sets deposition current below 200 A to avoid forming defects caused by high arc pressure. During the experiments, it was observed that when the deposition current was within the range from 200 to 350 A, the forming characteristics of the deposition beads varied from well-formed to slightly poor spreading, seriously poor spreading, and finally wire inserting with the growth of wire feed speed. However, when the deposition current was more than 350 A, the forming characteristics of the deposition beads turned from well-formed to wire inserting directly. The evolution of deposition bead forming characteristics and causes of forming defects are discussed following.

On one hand, the wire feed speed has an impact on the spreading process of deposition bead on the substrate. The main forces on the molten pool include gravity, arc pressure, and surface tension. The gravity and arc pressure promote the sinking down of the molten metal, while the surface tension

Fig. 2 Detection method and result of deposition bead outline data: **a** detection method, **b** original image, **c** point cloud data



prevents the molten pool from overflowing. Fig. 3a to d are the typical forming appearance of well-formed beads without any defects, and the contact angle between the substrate and the bead is smaller than 90 deg since the molten pool is able to reach a steady state with these forces and spread on the

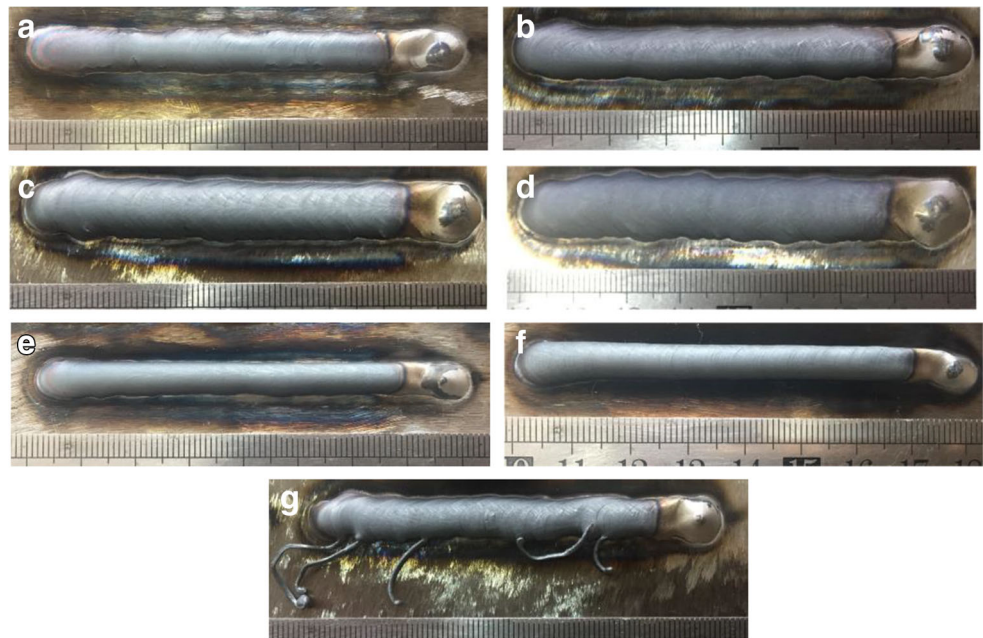
substrate. The outline of the well-formed bead is a curve smoothly connected with the substrate line.

If the wire feed speed grows further, more molten metal is fed into the molten pool, so the volume of molten pool increases. But it was noticed that the width of molten pool (the

Table 3 Forming characteristics with different deposition currents and wire feed speed

Exp. No.	Deposition current I (A)	Travel speed v (mm/s)	Wire feed speed vf (m/min)	Forming characteristic
1	200	3	1	Well-formed
2	200	3	1.5	Slightly poor spreading
3	200	3	2	Slightly poor spreading
4	200	3	2.5	Seriously poor spreading
5	200	3	3	Seriously poor spreading
6	200	3	3.5	Seriously poor spreading and wire inserting
7	250	3	1.5	Well-formed
8	250	3	2	Well-formed
9	250	3	2.5	Slightly poor spreading
10	250	3	3	Slightly poor spreading
11	250	3	3.5	Seriously poor spreading
12	250	3	4	Seriously poor spreading and wire inserting
13	300	3	2.5	Well-formed
14	300	3	3	Well-formed
15	300	3	3.5	Slightly poor spreading
16	300	3	4	Slightly poor spreading and wire inserting
17	350	3	3.5	Well-formed
18	350	3	4	Well-formed
19	350	3	4.5	Slightly poor spreading and wire inserting
20	400	3	4.5	Well-formed
21	400	3	5	Wire inserting
22	450	3	5	Well-formed

Fig. 3 Forming appearance of typical deposition beads, **a** Exp. No.7, **b** Exp. No.14, **c** Exp. No. 18, **d** Exp. No. 22, **e** Exp. No. 9, **f** Exp. No.11, **g** Exp. No. 16



distance between two feet of the bead) nearly did not change as the heat input to the substrate is constant, so that the surface tension makes the molten pool higher and plumper, thus the contact angle increases. When the contact angle is around 90 deg, the bead forming characteristic becomes slightly pool spreading as Fig. 3e. The outline of the slightly pool spreading bead seems discontinuous to the substrate line at the bead foot areas because these areas are nearly vertical to the line-structured laser, which decreases the density of the test point over there. For the multibead overlapping deposition process, the arc heat cannot approach to the former bead foot area, which will increase the risk of causing non-fusion defect. So it is better to avoid the appearance of the slightly pool spreading bead.

If the wire feed speed keeps on growing, the effect of gravity will be more remarkable than surface tension. The width of molten pool is still maintained, but the molten metal starts

sinking down, and extending along the transverse direction, which makes the contact angle bigger than 90 deg, and the distance between two feet is not yet the widest part of the bead. The line-structured laser can only project to the area above the widest part of the bead but cannot reach the area below that, so the detection contour is separated from the substrate line. In this case, the bead is seriously pool spreading as Fig. 3f, and it is scarcely possible to obtain a flawless deposition part.

On the other hand, the maximum allowable wire feed speed is limited by the arc heat. While the wire feed speed grows to a certain extent, the arc heat is insufficient to melt the wire in time. So the wire will crash on the bottom of the molten pool, then it will be bended and protrude out of the molten pool. Once the frizzy protruded wire contacts the twin electrodes, it will be melted and spread along the gap between the twin electrodes, and finally connects the twin electrodes together. Therefore, the electrodes will be polluted and the distribution of deposition current will be changed, resulting in an unstable process.

Thus, according to the experimental result in Table 3, the effect of wire feed speed and deposition current on forming characteristics was shown as Fig. 5. There are 3 zones in Fig. 5: well-formed zone, poor spreading zone, and wire inserting zone. Two boundary curves are respectively named after pool spreading curve and wire inserting curve. These two curves intersect at nearby 350 A.

The arc heat to melt the wire is a factor affecting the forming characteristics. The wire inserting curve in Fig. 5 reveals the ultimate ability of arc to melt the wire at various deposition currents from 200 to 450 A, which reflects the relationship between heat input and deposition rate. The arc

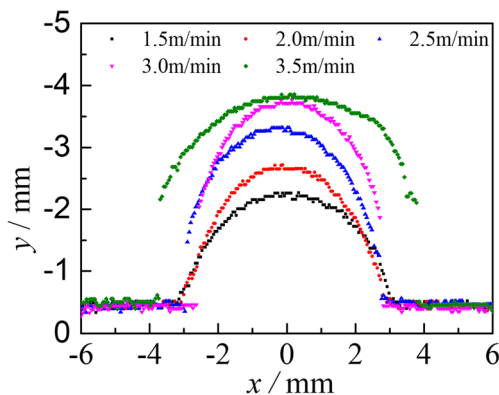


Fig. 4 The outlines of the beads deposited by 250 A at different wire feed speeds

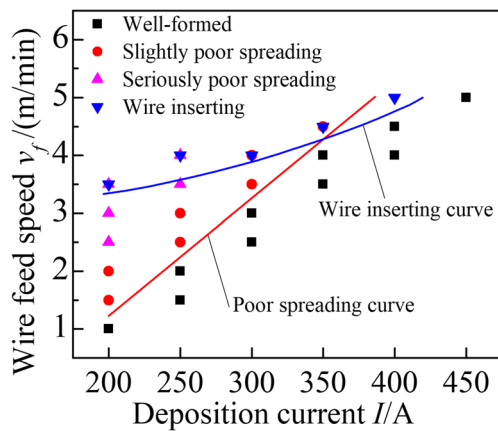


Fig. 5 The forming characteristics distribution with wire feed speed and deposition current

heat transferred to wire per unit time can be described by the following equation:

$$q = \eta UI \quad (1)$$

where η is the thermal efficiency of arc to heat the wire [18]. And U is the arc voltage, which is constant in this research. Figure 6 shows the arc shapes at different deposition currents, which were collected by Xiris-xvc1000 wide dynamic camera. It was found that the lower deposition current, the slenderer arc shape. Most of the arc zone is in contact with the wire at low deposition current, which is conducive to heat transfer. So the thermal efficiency of arc is high. With the increase of deposition current, the arc shape enlarges, which reduces the proportion of arc zone contacted with wire in total arc zone. The part of arc zone far away from the wire nearly does no help to melt the wire. It leads to the slightly decrease of thermal efficiency of arc. Thus, the change of thermal efficiency with deposition current is the reason that the heat input increased is not proportional to the increase of the melt speed of wire. But the thermal efficiency will not decrease indefinitely. As the convergence of the thermal efficiency when the current exceeds 300 A, the heat input increased is proportional to the increase of the melt speed of wire.

The arc heat to form the molten pool is also a factor affecting the forming characteristics. When the deposition current is low, the heat input to form the molten pool is also low. It narrows the molten pool and decreases the width of deposition

bead. In this case, the molten pool is easier to become higher and poor spreading with the growth of wire feed speed. When the deposition current is high, the molten pool gets wide enough to accommodate more molten metal, but the arc heat may not melt that much wire in time. So the wire was fed into the molten pool before melted, and the wire inserting defect appeared instead of poor spreading defect.

In order to improve robustness of results, the topmost square point of each column in Fig. 5 is chosen as the maximum allowable wire feed speed at each deposition current. A piecewise linear function with a demarcation point of 350 A was employed to describe the relationship between the maximum allowable wire feed speed and deposition current. It satisfies the following:

$$v_{f\max} = \begin{cases} 0.02I - 3 & , 200A < I \leq 350A \\ 0.01I + 0.5 & , 350A < I < 450A \end{cases} \quad (\text{m/min}) \quad (2)$$

In the following experiments, the wire feed speed and deposition current are matched according to Eq. (2).

3.2 The feasible travel speed ranges at each deposition current

The experiment results were shown as Table 4. The forming characteristics mainly include well-formed, well-formed but exceeding limited height, and discontinuous. The outlines of beads deposited by 350 A deposition current at different travel speeds were given as Fig. 7. It was found that the width and height all grew with the decrease of travel speed, because the arc duration per unit length got longer, which increased the total heat input and molten metal input. But with the highest point of molten pool approaching to the tips of twin electrodes, once the interferences of the deposition process give it an upward fluctuation, short circuit will happen so that the deposition bead has tungsten inclusion defect and the electrodes are polluted as well. Besides, the large molten pool leads to serious heat sink, which is harmful to properties. So in this work, 3 mm was set as the limited height of a deposition bead, and the deposition parameters to obtain the exceeding limited height bead are forbidden to use for the sake of avoiding the risk of short circuit. It determines the lower limit of travel speed. Conversely, when the travel speed is too fast,

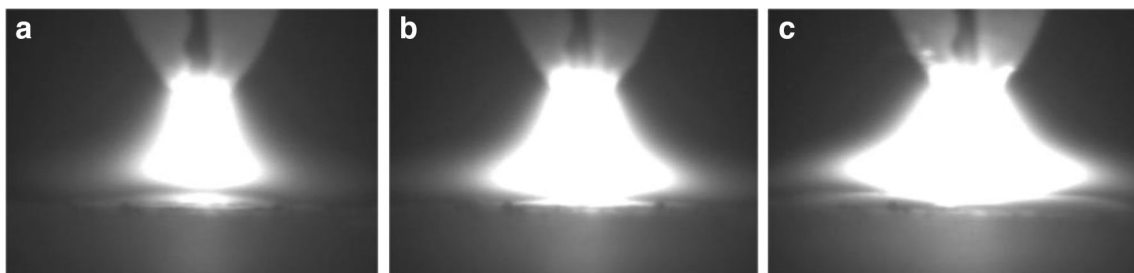


Fig. 6 The arc shapes of different deposition currents **a** 200 A, **b** 350 A, **c** 450 A

Table 4 Forming characteristics with different deposition currents and travel speeds

Exp. No.	Deposition current I (A)	Travel speed v (mm/s)	Wire feed speed v_f (m/min)	Forming characteristic
1	200	1	1	Well-formed but exceeding limited height
2–5	200	1.5, 2, 3, 4	1	Well-formed
6	200	5	1	Discontinuous
7–8	250	1.5, 2	2	Well-formed but exceeding limited height
9–12	250	2.5, 3, 4, 5	2	Well-formed
13	250	6	2	Discontinuous
14	300	2.5	3	Well-formed but exceeding limited height
15–18	300	3, 4, 5, 6	3	Well-formed
19	300	7	3	Discontinuous
20	350	2.5	4	Well-formed but exceeding limited height
21–25	350	3, 4, 5, 6, 7	4	Well-formed
26	350	8	4	Discontinuous
27	400	2.5	4.5	Well-formed but exceeding limited height
28–33	400	3, 4, 5, 6, 7, 8	4.5	Well-formed
34	400	9	4.5	Discontinuous
35	450	2.5	5	Well-formed but exceeding limited height
36–42	450	3, 4, 5, 6, 7, 8, 9	5	Well-formed
43	450	10	5	Discontinuous

the arc heat input to the substrate is too small to form the molten pool. In this case, the bead is made up of a series of droplets, so its forming characteristic is discontinuous. It determines the upper limit of travel speed. The forming appearances of discontinuous beads were given as Fig. 8.

Figure 9 presents the feasible travel speed ranges, and it is also the process window of twin electrode GTA-AM. It was found that the upper limit curve increases with deposition current while the lower limit curve first increases and then converges. For the upper limit curve, as the heat input per unit time raises with the deposition current, the energy accumulation rate increases. Thus, it needs less time to melt substrate and forms a molten pool, which means that the travel speed to get the well-formed bead could be faster. For the lower limit

curve, when the deposition current reaches a higher level, the deposition bead is difficult to get higher as the following reasons: (i) The growth rate of wire feed speed with deposition current decreases after 350 A as Eq. (2), but the width of molten pool is still grow as usual, so the quantity of molten metal is not enough to make the bead grow higher. And (ii) the increasing of gravity promotes the molten pool sinking down and makes the molten pool plumper, instead of higher. So the lower limit curve first increases and then converges.

In comparison with traditional GTA-AM process, the defects such as undercutting and humping did not appear during the twin electrode GTA-AM process. High arc pressure and high travel speed are the necessary conditions of undercutting and humping. For the traditional GTA-AM technology at high

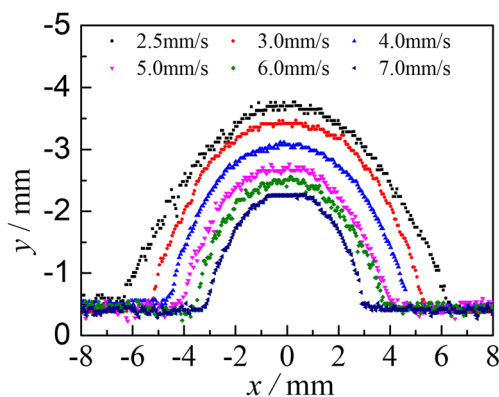


Fig. 7 The outline of the beads deposited by 350 A at different travel speeds



Fig. 8 Forming appearances of discontinuous beads, **a** Exp. No. 6, **b** Exp. No. 19

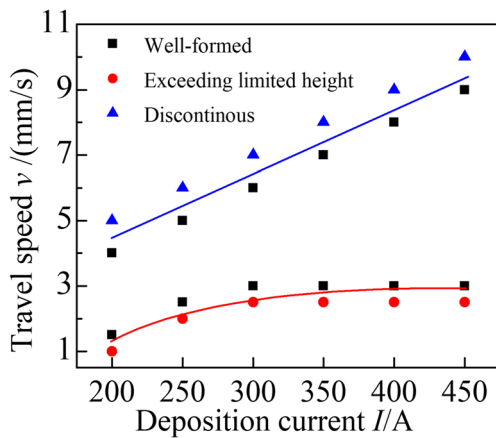


Fig. 9 The feasible ranges of travel speed

deposition current and high travel speed, the molten metal in the front of molten pool is pushed backward by arc pressure and leaves a liquid film below the arc, and the arc moves away from the above of liquid film quickly. So the liquid film will be frozen into solid and prevent the flow of molten pool, which results in the inhomogeneous deposition bead [19]. But for the twin electrode GTA-AM technology, the coupled arc pressure is much lower than that of traditional gas tungsten arc with single electrode, which weakens the motion force to push the molten metal backwards and prevents the forming of liquid film. So it is feasible for twin electrode GTA-AM to deposit well-formed bead at high deposition current and high travel speed. The maximum travel speed is up to 9 mm/s when the deposition current is 450 A, and the wire feed speed is 5 m/min.

4 Experimental validation of twin electrode GTA-AM

4.1 Single-layer multibead component

A single-layer component with 5 overlapping beads was first deposited by twin electrode GTA-AM technology. As recommended by the process window proposed in this paper, the

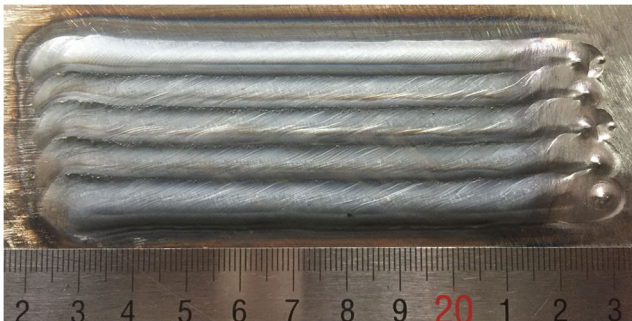


Fig. 10 Overview of the single layer component deposited by twin electrode GTA-AM

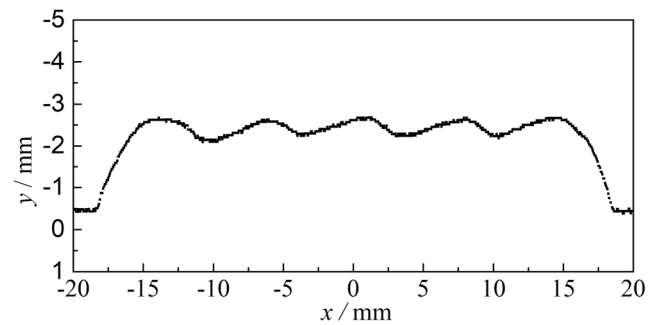


Fig. 11 The cross section outline of the deposited single layer

following deposition parameters were set: 450 A deposition current, 5 m/min wire feed speed, and 5 mm/s travel speed. By using the selected deposition parameters, the geometries of the deposited beads were measured as 2.12 mm height and 10.05 mm width. The applied overlapping distance was 7 mm. Accordingly, the expected width of the layer was 38.05 mm. The deposition layer was shown as Fig. 10, and the aggregated cross-section outline was given as Fig. 11. The measured width of the layer was 37.56 mm. The average height of each bead in this layer was 2.16 mm. It can be seen that this deposition layer was well-formed without any forming defect, and the expected geometries was achieved.

4.2 Multilayer multibead component

In order to further validate the feasibility of fabricating metal components with twin electrode GTA-AM, a forming experiment of multilayer multibead block component was conducted with the deposition parameters mentioned in section 4.1. This structure includes 9 layers, and each layer has 3 overlapping beads. The deposition direction of each bead is the same. The deposition sequence in each layer is from the middle to both sides. The geometries of the target component were 100 mm length, 24 mm width, and 19 mm height. The

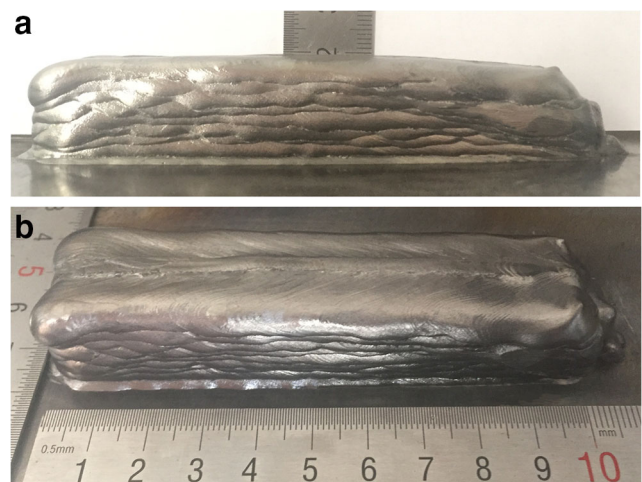


Fig. 12 Overview of the multilayer multibead component deposited by twin electrode GTA-AM, **a** side view, **b** global view

Table 5 Comparison of the present work with some typical studies on deposition rate

Authors	Method	Filling material	Wire feed speed	Deposition rate
Colegrove et al. [21]	GMA-AM	0.8-mm diameter wire of ER70S-6	10 m/min	2.4 kg/h
Xiong et al. [22]	GMA-AM	1.2-mm diameter wire of H08Mn2Si	6 m/min	3.2 kg/h
Yilmaz and Ugla [23]	GTA-AM	0.8-mm diameter wire of ER308LSi	3.5 m/min	0.8 kg/h
Iván et al. [10]	GTA-AM	1.2-mm diameter wire of AISI 316 L	Not mentioned	1.5 kg/h
This paper	Twin electrode GTA-AM	1.2-mm diameter wire of H08Mn2Si	5 m/min	2.7 kg/h

deposited block component was shown as Fig. 12. Forming defects did not occur during the deposition process. A common problem of WAAM [20] also arises in twin electrode GTA-AM process, the arc-striking ends were higher than the middle part and the arc-extinguishing ends was lower than the middle part. At these two ends, the arc length deviated from the set value of 5 mm, which results in the change of process stability and affect the forming characteristics. Except the arc-striking and arc-extinguishing ends, the deposited block component is well-formed. The measured width of this component is 23.52 ± 1 mm. The measured height of this component is 19.14 ± 0.3 mm. The expected geometries were achieved.

According to material balance rule, deposition rate (DR) is equal to the wire feed mass per unit time, and it can be calculated with the wire feed speed v_f , the wire diameter d , and the density of wire ρ as:

$$DR = \pi \rho d^2 v_f / 4 \quad (3)$$

Table 5 listed the present work and some recent studies on traditional WAAM technology using similar filling materials. The deposition rate in Table 5 was given by the author directly, or calculated with the values in corresponding articles according to Eq. (3). The maximum deposition rate of twin electrodes GTA-AM for mild steel is up to 2.7 kg/h at the experimental conditions described in section 2. The result shows that deposition rate of twin electrodes GTA-AM is almost twice as much as that of traditional GTA-AM and is almost at the same level with GMAAM. Thus, employing the heat source of twin electrode gas tungsten arc is an effective method to improve the deposition rate of GTA-AM.

5 Conclusions

- 1) The feasibility of twin electrode GTA-AM to deposit the well-formed bead at high deposition currents up to 450 A has been validated. It is able to avoid undercutting and humping defects caused by high arc pressure.
- 2) With the growth of wire feed speed, the connect angle between deposition bead and substrate increases. The maximum allowable wire feed speed to ensure the

deposition bead well-formed at each deposition current is explored by experiments. The wire feed speed higher than that will lead to poor spreading defect or wire inserting defect.

- 3) The width and height of deposition bead both decrease with the growth of travel speed. The feasible travel speed range at each deposition current with its maximum allowable wire feed speed is experimentally found. It can reach 9 mm/s at the deposition current of 450 A.
- 4) The verification experiment has proved that twin electrodes GTA-AM is able to fabricate metal components without defects at a high deposition rate. Its deposition rate is up to 2.7 kg/h, which is almost twice as much as that of traditional GTA-AM, and is almost at the same level with GMA-AM.

Funding information This work was supported by the National Key R&D Program of China (2018YFB1105800).

References

1. Li Y, Han Q, Zhang G, Horváth I (2018a) A layers-overlapping strategy for robotic wire and arc additive manufacturing of multi-layer multi-bead components with homogeneous layers. Int J Adv Manuf Technol 96:3331–3344
2. Ma G, Zhao G, Li Z, Yang M, Xiao W (2019) Optimization strategies for robotic additive and subtractive manufacturing of large and high thin-walled aluminum structures. Int J Adv Manuf Technol 101:1275–1292
3. Williams S, Martina F, Addison A, Ding J, Pardal G, Colegrove P (2016) Wire + arc additive manufacturing. Mater Sci Technol 32: 641–647
4. Li Y, Huang X, Horváth I, Zhang G (2018b) GMAW-based additive manufacturing of inclined multi-layer multi-bead parts with flat-position deposition. J Mater Process Technol 262:359–371
5. Li Y, Han Q, Horváth I, Zhang G (2019) Repairing surface defects of metal parts by groove machining and wire + arc based filling. J Mater Process Technol 274:116268
6. Shen C, Pan Z, Cuiuri D, Roberts J, Li H (2016) Fabrication of Fe-FeAl functionally graded material using the wire-arc additive manufacturing process. Metall Mater Trans B 47:763–772
7. Wang F, Williams S, Colegrove P, Antonysamy A (2013) Microstructure and mechanical properties of wire and arc additive manufactured Ti-6Al-4 V. Metall Mater Trans A 44:968–977

8. Bai J, Fan C, Lin S, Yang C, Dong B (2016) Effects of thermal cycles on microstructure evolution of 2219-Al during GTA-additive manufacturing. *Int J Adv Manuf Technol* 87:2615–2623
9. Geng H, Li J, Xiong J, Xin L, Zhang F (2017) Optimization of wire feed for GTAW based additive manufacturing. *J Mater Process Technol* 243:40–47
10. Taberero I, Paskual A, Álvarez P, Suárez A (2018) Study on arc welding processes for high deposition rate additive manufacturing ☆. *Procedia Cirp* 68:358–362
11. Ding D, Pan Z, Cuiuri D, Li H (2015) Wire-feed additive manufacturing of metal components: technologies, developments and future interests. *Int J Adv Manuf Technol* 81:465–481
12. Zhu L, Li J, Luo Y, Han J, Zhang C, Xu J, Chen D (2018) Characteristics of metal droplet transfer in wire-arc additive manufacturing of aluminum alloy. *Int J Adv Manuf Technol* 99: 1521–1530
13. Leng X, Zhang G, Wu L (2006a) Experimental study on improving welding efficiency of twin electrode TIG welding method. *Sci Technol Weld Join* 11:550–554
14. Kobayashi K, Nishimura Y, Iijima T, Ushio M, Tanaka M, Shimamura J, Ueno Y, Yamashita M (2004) Practical application of high efficiency twin-arc TIG welding method (Sedar-TIG) for Pclng storage tank. *Weld World* 48:35–39
15. Zhang G, Leng X, Wu L (2006) Physics characteristic of coupling arc of twin-tungsten TIG welding. *Trans Nonferrous Metals Soc China* 16:813–817
16. Leng X, Zhang G, Wu L (2006b) The characteristic of twin-electrode TIG coupling arc pressure. *J Phys D Appl Phys* 39: 1120–1126
17. Wang X, Fan D, Huang J, Huang Y (2015) Numerical simulation of arc plasma and weld pool in double electrodes tungsten inert gas welding. *Int J Heat Mass Transf* 85:924–934
18. Gonçalves L C, Vilarinho O, Scotti A, Guimarães G (2006) Estimation of heat source and thermal efficiency in GTAW process by using inverse techniques. *J Mater Process Technol* 172:42–51
19. Gu Y, Hua X, Ye D, Li F, Ma X, Xu C (2017) Numerical simulation of hump suppression in high-speed triple-wire GMAW. *Int J Adv Manuf Technol* 89:727–734
20. Hu Z, Qin X, Shao T, Liu H (2018) Understanding and overcoming of abnormality at start and end of the weld bead in additive manufacturing with GMAW. *Int J Adv Manuf Technol* 95:2357–2368
21. Colegrove P, Coules H, Fairman J, Martina F, Kashoob T, Mamash H, Cozzolino L (2013) Microstructure and residual stress improvement in wire and arc additively manufactured parts through high-pressure rolling. *J Mater Process Technol* 213:1782–1791
22. Xiong J, Zhang G, Gao H, Wu L (2013) Modeling of bead section profile and overlapping beads with experimental validation for robotic GMAW-based rapid manufacturing. *Robot Comput Integr Manuf* 29:417–423
23. Yilmaz O, Uglu A (2017) Microstructure characterization of SS308LSi components manufactured by GTAW-based additive manufacturing: shaped metal deposition using pulsed current arc. *Int J Adv Manuf Technol* 89:13–25

Publisher's note Springer Nature remains neutral with regard to jurisdictional claims in published maps and institutional affiliations.